ARTICLE
JOURNAL OF UNIVERSITY OF BABYLON For ENGINEERING SCIENCES (JUBES)
Vol.29, No.2.| 2021

"Optimization of Radio Frequency Sputtering of Graphite on Nitinol "

Zaineb Fadhil Kadhim **Ekbal Mohammed Saeed** **Haider A.H. Al-Jubouri**

Collage of Engineering Materials, Department of Metallurgical Engineering, University of Babylon

E-mail: mat.zainab.fadhil@uobabylon.edu.iq

Received:	**10/8/2021**	**Accepted:**	**13/9/2021**	**Published:**	**12/10/2021**

Abstract

The unique performance offerings of Ni-Ti alloys which involve the shape memory effect, super elasticity and biocompatibility have led to widespread acceptance of these alloys as valuable engineering materials. Deposition thin film from graphite target on nitinol by using radio frequency sputtering as physical vapor deposition method . Determination the improvement in hardness, wear rate, roughness, corrosion rate and cell viability before and after deposition. Three values of radio frequency sputtering as (200W, 400W, 600W) are used. The deposited film is considered as diamond like carbon DLC depending on peaks of Raman spectroscopy. DLC had good characteristics as antibacterial property, low friction coefficient, high wear resistance and good corrosion resistance. High power led to high Vickers hardness as 657 with low specific wear rate as $7.34*10^{-8}$g/cm. High corrosion resistance achieved after 400W as 0.001mm/y and high cell viability as 93.11%. The optimized results from genetic algorithm with fuzzy inference system pointed as power 222W, Vickers hardness as 666,corrosion current density 0.138,and cell viability as 88.8.

Keywords: Nitinol alloy, Sputtering, Radio frequency, Deposition, Target, Graphite

1. Introduction:

Surface engineering proposes remarkable methods to change the surface and near-surface region of a material so as to enhance its properties in terms of surface sensitivity[1]. The advanced techniques are chemical vapor deposition CVD, physical vapor deposition PVD, spraying, and surface modification by surface melting, heat treatment, and ion implantation [2].

Physical Vapor Deposition is a thin film deposition procedure whereby the coating is grown on the substrate atom by atoms. PVD encompasses the material to atomize and vaporize from a solid source, also known as target. It is the most important applications of vacuum systems to produce thin films [3], [4].

The sputtering is a method of PVD. The advantages of it are: using unlimited materials as source and film as (metals, semiconductors, insulators, alloys, compounds),environmentally friendly processing, high degree of film adhesion and uniformity of thickness over large areas. The entire surface of target is the source of deposition [5],[6].

Carbon is the fundamental element in all recognized living systems and without it life could not exist. It is the fourth abundant chemical element in the universe by mass after hydrogen, helium and oxygen. There are many phases of carbon deposited by using physical vapour deposition and chemical vapour deposition [7].

The optimization is the process of calculating the best design or representation. This procedure can be applied in all fields of engineering , medicine, chemical and physical applications[8]. The basis of the

مجلة جامعة بابل للعلوم الهندسية

ISSN: 2616 - 9916 | www.journalofbabylon.com | Journal.eng@uobabylon.edu.iq | info@journalofbabylon.com

genetic algorithm is the Darwinian theory of nature selection. The genetic algorithm is considered as an evolutionary algorithm [9].

2.Materisals and Methods:

The equiatomic alloy of Ni-Ti was made from (50%Ni- 50%Ti) by atomic percent in powder metallurgy. All specimens heating with rate $10℃/min$ to 950°C and soaking for 7 hours with slow cooling to room temperature to form nitinol alloy in tube furnace with Ar gas. They were mechanically polished on every side to a mirror finish, ultrasonically cleaned, and dried. Radio frequency (RF) sputtering was done by a machine which was made in Germany (Bestec company).The target for sputtering was provided from Changsha Xinkang Advanced Materials Co. Ltd. The diameter of graphite target is 4.8 cm (48mm) and its thickness is 0.5cm (5mm) with a purity rate of 98.9999%. The base pressure was $2 * 10^{-5}$ mbar. After emptying the chamber from air, the flow of (Ar) gas with 22 sccm (standard cubic centimeters per minute, unit of mass flow rate)and the pressure during depositions is $3*10^{-3}$ mbar. The distancing span that separated the carbon target and nitinol substrate was 11.5 cm. The substrate was heated gradually to reach a balance temperature of 120°C. The thickness monitor was used to control the thickness of thin film as 150nm. Three powers used as (200W, 400W, 600W).

The Raman Teksan model P50C0R10 using a green light of 532 nm of Nd:YAG (neodymium yttrium aluminium garnet) laser used for specimens after deposition. Atomic force micrograph (AFM) used in observing the surface roughness as well as the topography of the specimens. The micro hardness of the specimens was measured at an applied force of 200g with a duration time of 10 sec. The adhesive wear test and friction coefficient calculated by using pin on disc method. The value of load is 15N with a rotation speed of 250rpm and wear track radius as 5mm.The manner is repeated until reached to 60min. specific wear rate is calculated as the following[10]:

Specific wear rate $=\frac{\Delta w}{S}$ (g/cm) ----Eq.(1)

Where:

$\Delta w = weight\ \ loss\ (g)$

S=sliding distance (471m)

S=sliding velocity (m/sec)*time (sec) ----Eq.(2)

Sliding velocity $=\frac{\pi DN}{60*1000}$ -----Eq.(3)

Where :

D=wear track diameter selected (10mm)

N=speed of rotation disk (250rpm)

Electrochemical test is used for all specimens in ringer solution. The temperature of solution fixed at 37℃ and the pH of ringer solution is 7.4. Each 100 ml of body fluid ringer includes: sodium chloride 0.860 g, potassium chloride 0.03 g and calcium chloride 2H2O 0.33g. Tafel extrapolation method has been employed in measuring the corrosion rate. There were three electrodes in in this cell: the working electrode represented the specimen, whereas the counter and reference electrodes represented the platinum and saturated calomel electrodes, respectively. The value of corrosion rate can be determined from the data of this test according to [ASTM G102] as follows [11],[12]:

ISSN: 2616 - 9916 | www.journalofbabylon.com | Journal.eng@uobabylon.edu.iq | info@journalofbabylon.com

$$corrosion\ rate = K \times i_{corr} \times \frac{EW}{D}$$ -----Eq.(4)

Where:

Corrosion rate = (mm/year)

K = 3.27×10^{-3} mm g/$\mu A\ cm\ year$

D= material density (g/cm^3)

i_{corr}= corrosion current density($\mu A/cm^2$)

$$i_{corr} = \frac{I_{corr}}{A}$$ -----Eq.(5)

Where:

i_{corr} = the corrosion current density in $\mu A/cm^2$

I_{corr} = the total current density in µA

A = the exposed surface area in cm^2

EW= equivalent weight

EW=1/Q ----- Eq. (6)

$$Q=\sum_{i=1}^{n} \frac{n_i f_i}{w_i}$$ ----Eq. (7)

Where:

f_i=mass fraction of the i^{th} element within alloy

n_i=valance of i^{th} element of alloy

w_i = atomic weight of the i^{th} the element within alloy

The MTT which means [Dimethyl-thiazol-diphenyl-tetrazolium-bromide] test is based on cytotoxicity assay. The cytotoxicity of research reagents was measured by detect cells that remain viable and were capable of proliferation, through determining the amount of MTT-formazan produced by reducing MTT-dye by live cells. Then, the MTT-based cytotoxicity assay protocol was completed for assessing the impact of metals on cell line. Normal cells of Madian Darpy Canine Kidney(MDCK) were used in this test. The absorbance was determined using an Elisa reader at a wavelength of 570 nm. After all tests of nitinol specimens before and after deposition ,the optimization method applied in MATLAB (matrix laboratory) version 7. To find optimized results for RF sputtering used the combination of genetic algorithm and fuzzy inference system.

3.Results and Discussion:

3.1 Raman spectroscopy:

a- 200W:

The first peak of this deposited film at 200W lower than $200cm^{-1}$. The low frequency region between $(100\text{-}300)cm^{-1}$ relates to radial breathing modes(RBM). This peak is not limited to carbon nanotubes but appears in other phases [13]. The Important range of carbon phases in Raman spectroscopy was between $(1300\text{-}3000)cm^{-1}$ as shown in Figure (1-a).The D and G peak represented at $1364cm^{-1}$ and $1558cm^{-1}$. This

ISSN: 2616 - 9916 | www.journalofbabylon.com | Journal.eng@uobabylon.edu.iq | info@journalofbabylon.com

مجلة جامعة بابل للعلوم الهندسية
ISSN: 2616 - 9916 | www.journalofbabylon.com | Journal.eng@uobabylon.edu.iq | info@journalofbabylon.com

deposited film after RF sputtering was diamond like carbon DLC. It was example of wide distribution of the bond angles with an admixture of sp^2 and sp^3 crossing as in [14].

b- 400W:

The spectrum of a carbon deposited with RF sputtering reveals in Figure (1-b). The D-band represented at 1354cm-1 and G band showed at 1569cm-1. The G band matches to the uniform E2g C–C stretching fashion in graphite-like materials, while the D band refers to bond angle disturbance in the graphite-like micro domains influenced by sp3 bonds [15].

c- 600W:

The Raman spectra of deposited film represents in Figure(1-c). Two peaks of G band and D band were very clear in this spectrum. The height of peak rely on the parameters of the deposition and time of it. The high peak of G band referred to decrease in disordered of amorphous carbon. D and G peaks were found at 1350cm-1 and 1558cm-1 respectively. The G band describes the graphitic like layers of sp2 micro domains bond stretching of any couple of sp2 for each chains and rings [16]. The D band describes the bond angle disturbance in the sp2 graphite like micro domains stimulated by the connecting with sp3 carbon atom (breathing fashions of sp2 atoms in ring) as in [16].

The location of D band, G band and ID/IG express in table (1). The differences in time of deposition and energy applied in RF sputtering effected on the structure of film deposition . The ratio of ID/IG after 200 W and 600W was the same and lower than the ratio after 400 W as shown in Figure (2).

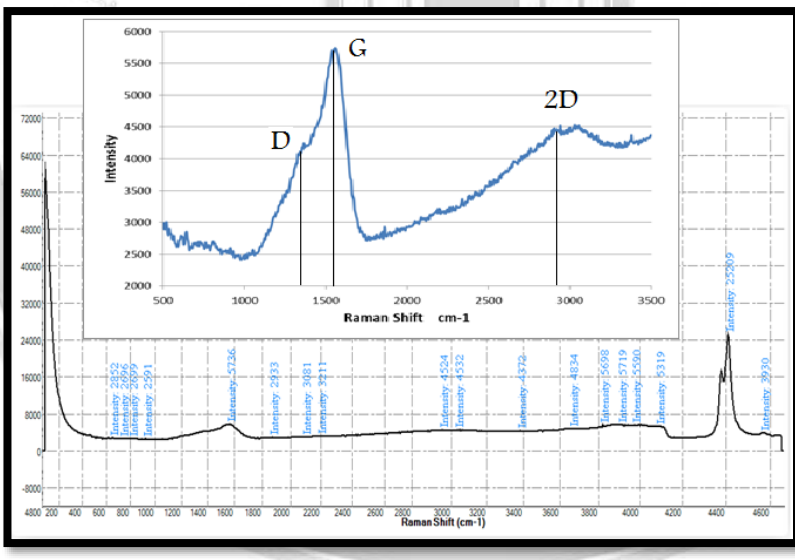

a

ARTICLE
JOURNAL OF UNIVERSITY OF BABYLON For ENGINEERING SCIENCES (JUBES)
Vol.29, No.2.| 2021

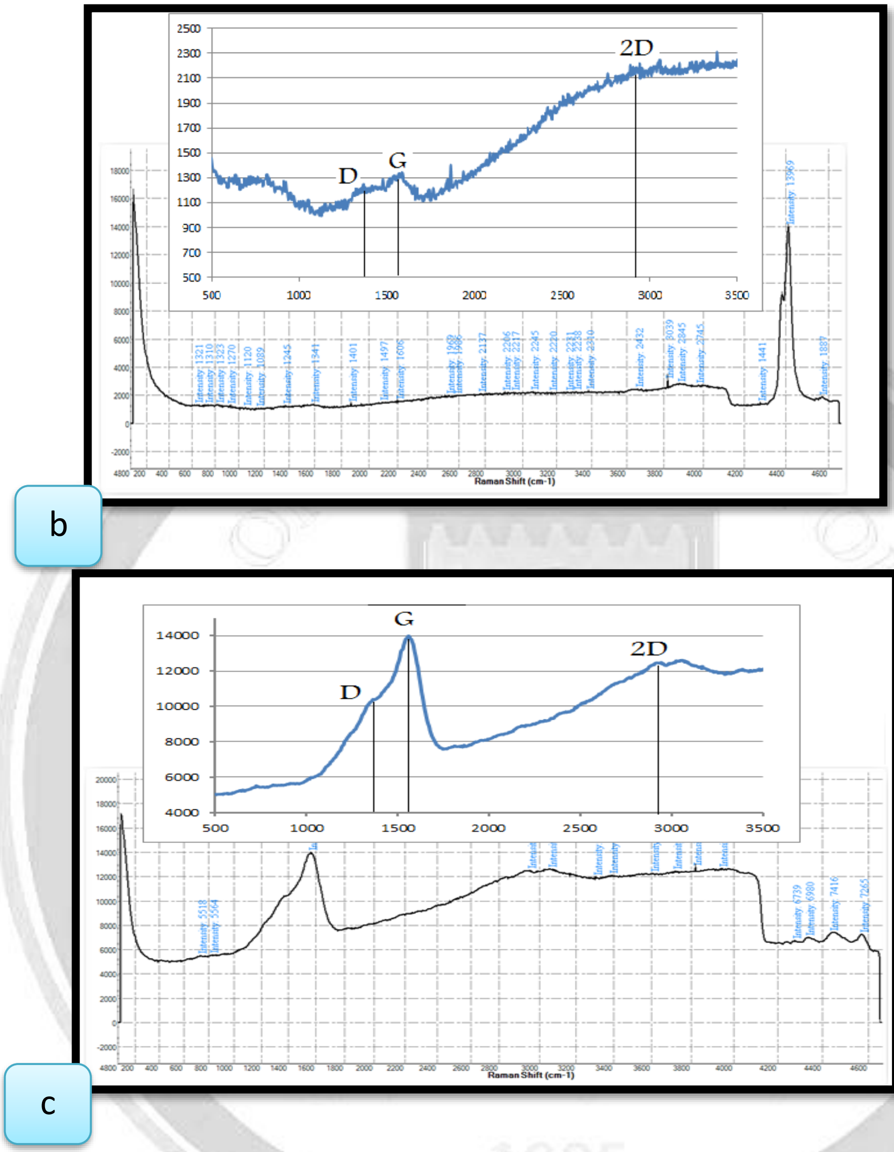

Figure (1): Raman spectra of deposited film on nitinol after RF Sputtering :9a)200W, (b)400W, (c) 600W

Table (1): The data of deposition time , positions of bands and ID/IG

Power (W)	RF Sputtering		
	200	400	600
Time of deposition (min)	170	150	120
G-Band position (cm^{-1})	1558	1569	1558
D-Band-position (cm-1)	1364	1354	1350
ID/IG	0.739	0.911	0.73

ISSN: 2616 - 9916 | www.journalofbabylon.com | Journal.eng@uobabylon.edu.iq | info@journalofbabylon.com

JOURNAL OF UNIVERSITY OF BABYLON For ENGINEERING SCIENCES (JUBES)
Vol.29, No.2.| 2021

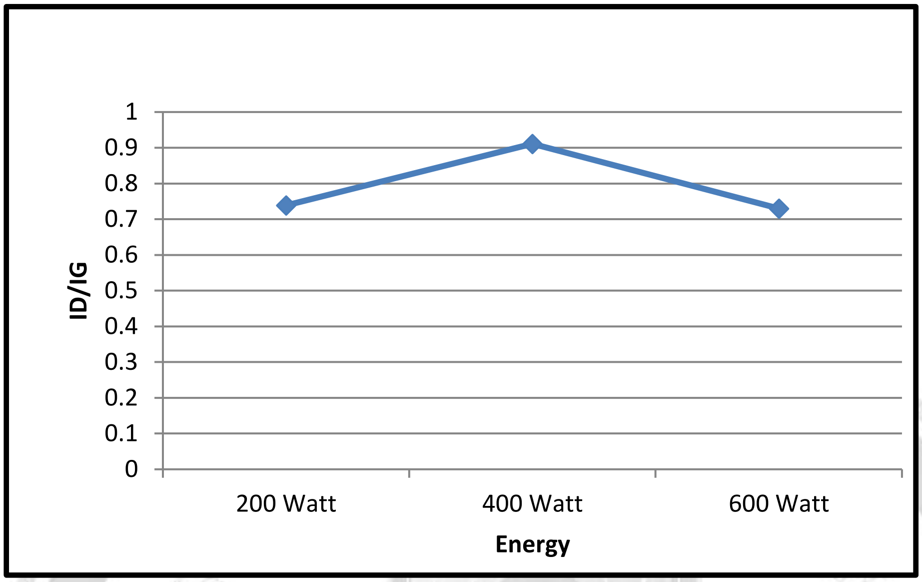

Figure (2): ID/IG of deposited film on nitinol after RF sputtering

3.2 Atomic Force Micrograph AFM: The scanned area by AFM for specimens after RF sputtering in ($3\mu m$ *$3\mu m$).The first specimen is examined as shown in Figure (3) which represents the roughness of bare as Ra=0.129µm. The morphology and topography of the specimens after RF sputtering reveals in Figure(3). They had roughness as (0.228µm, 0.224µm, 0.222μm)after (200W, 400W, 600W). The decreasing in the roughness with increasing power due to high power lead to high heat to nucleation and growth the DLC as in **[17].**

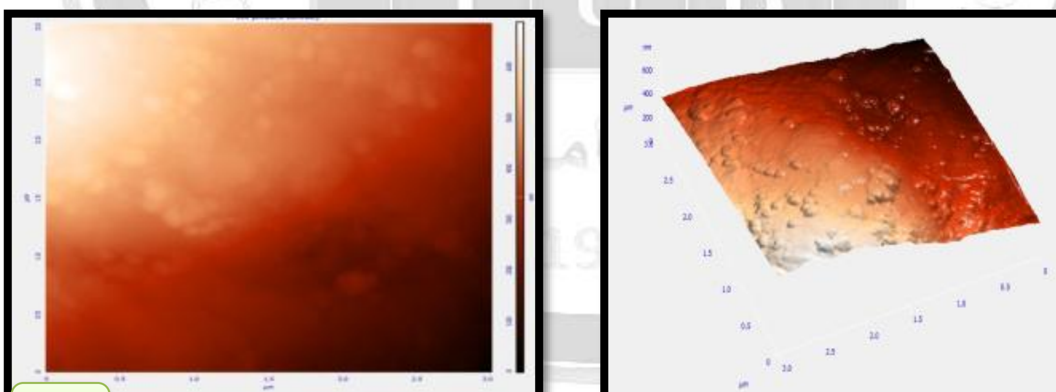

a

مجلة جامعة بابل للعلوم الهندسية
ISSN: 2616 - 9916 | www.journalofbabylon.com | Journal.eng@uobabylon.edu.iq | info@journalofbabylon.com

ISSN: 2616 - 9916
www.journalofbabylon.com | Journal.eng@uobabylon.edu.iq | info@journalofbabylon.com
مجلة جامعة بابل للعلوم الهندسية

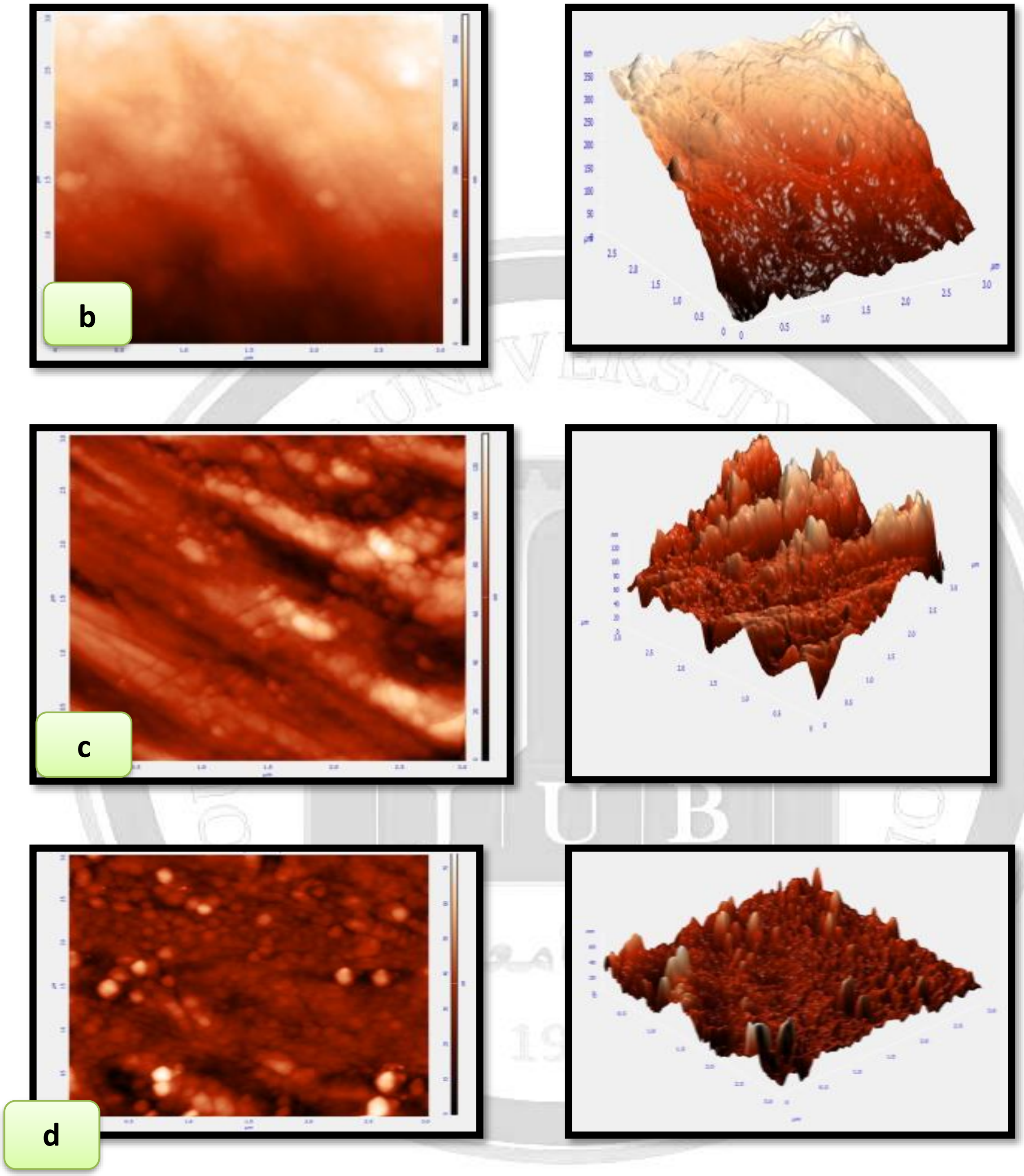

Figure (3): AFM in 2D and 3D after RF : (a)bare, (b)200W, (c)400W, (d)600W

3.3 Vickers Hardness:

The micro Vickers hardness of the bare specimen was 315. The coating hardness affected by some competing factors, such as microstructure, surface roughness, grain size, residual stress[18].Vickers hardness of specimens after RF sputtering increased with increasing the power as in Figure (4). The maximum hardness after 600 W is 657. The hardness is strongly dependent on the morphology of coating , for compact deposition in high power induced highest hardness as in [17; 19].

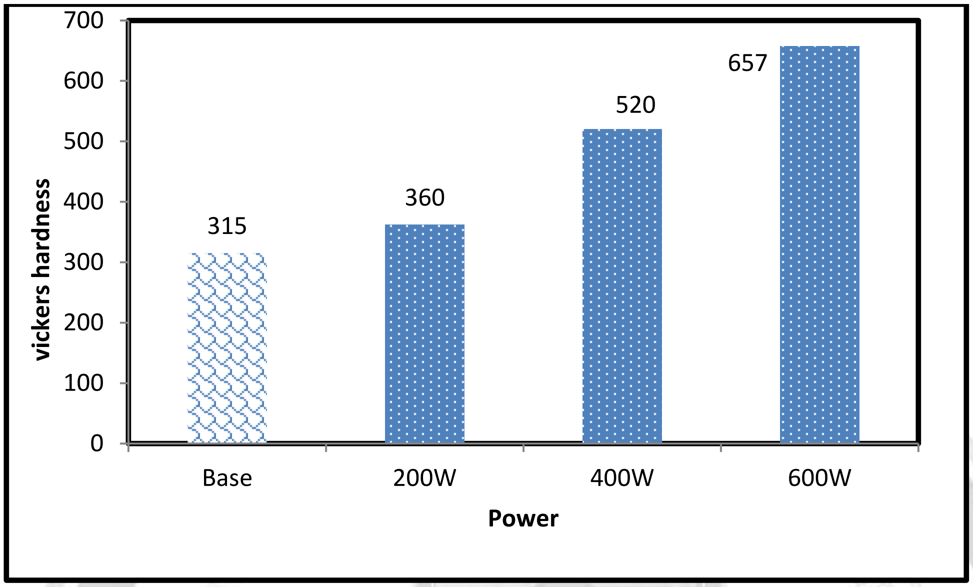

Figure (4): Vickers Hardness of deposited film on nitinol after RF sputtering

3.4 Wear Test :

The wear rate is a characteristic property for all materials specially biomaterials. The nitinol alloy which represents the bare specimen had the greatest wear rate by comparing with others after deposition which led to bad resistance to wear. The wear rate of deposited film after RF sputtering decreased as shown in Figure (5). The minimum value of wear rate was 2.3×10-8 g/cm after 200W.The wear rate increased with increasing the hardness of specimens as in [20].DLC films were known to exhibit low friction in various sliding condition ,which found to be attributed to a sliding induced graphitization. The graphitization resulted in the generation of nano scale tribofilms having sp2 type chemical bonding as in [21]. The specimen after power 600 W had the highest hardness, highest wear rate and highest coefficient of friction among others after RF sputtering and this result was compatible to [17]. Lowest surface roughness induced a higher friction coefficient as in [20].

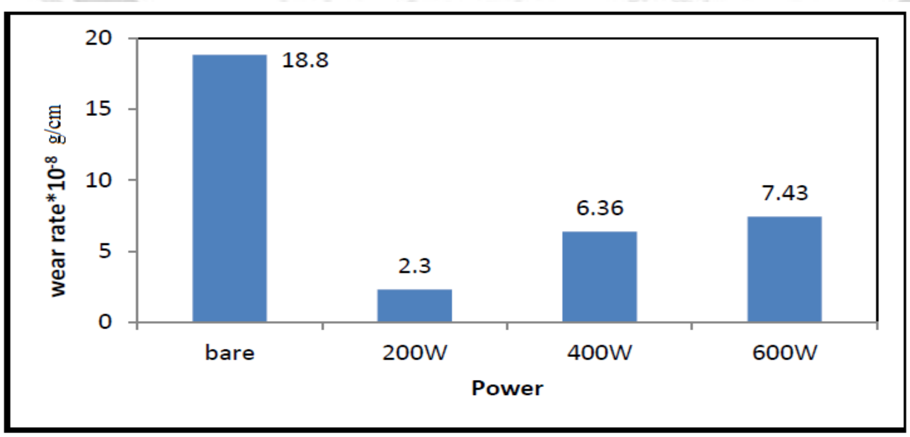

Figure (5): Wear rate of deposited film on nitinol after RF

ISSN: 2616 - 9916 | www.journalofbabylon.com | Journal.eng@uobabylon.edu.iq | info@journalofbabylon.com

ARTICLE
JOURNAL OF UNIVERSITY OF BABYLON
For ENGINEERING SCIENCES (JUBES)
Vol.29, No.2.| 2021

sputtering of graphite

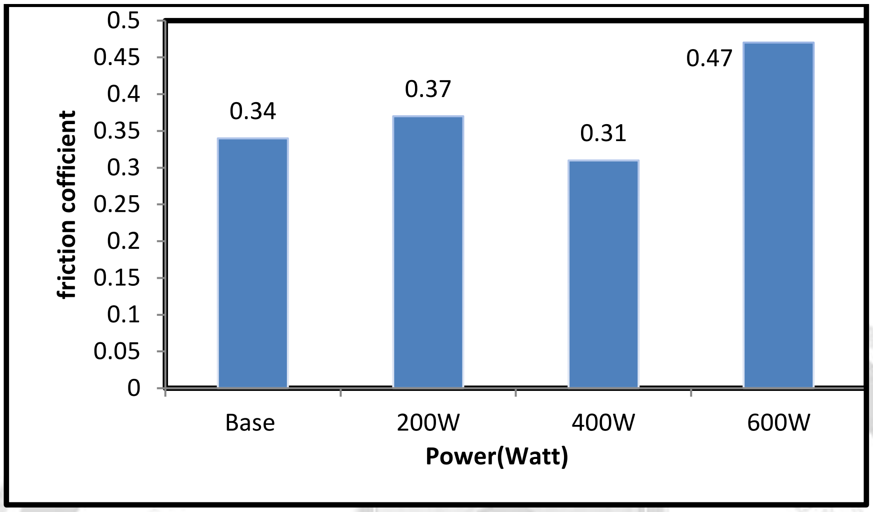

Figure (6): Friction coefficient of deposited film on nitinol after RF sputtering of graphite

3.5 Corrosion Test :

The nitinol alloy has resistance to corrosion because the nature of Ni and Ti. Tafel extrapolation of the bare and specimens after RF sputtering are represented in Figure(7). Figure (8) reveals the corrosion rate of specimens after RF sputtering. The corrosion rate of the bare specimen was 0.04 mm/y They had small corrosion rate as 0.0138m/y,0.001mm/y and 0.0152mm/y at 200W,400Wand 600 W respectively. The minimum rate of corrosion was represented by specimen deposited at 400W. The packing of film deposited by RF sputtering leads to decreasing the corrosion rate to low value than the bare of nitinol.

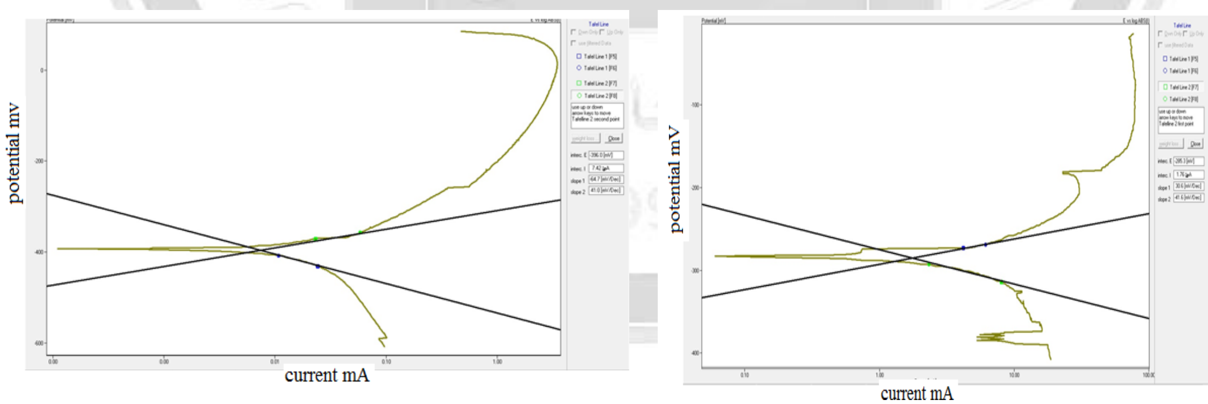

(a)bare

(b)200RF

ISSN: 2616 - 9916
www.journalofbabylon.com | Journal.eng@uobabylon.edu.iq | info@journalofbabylon.com
مجلة جامعة بابل للعلوم الهندسية

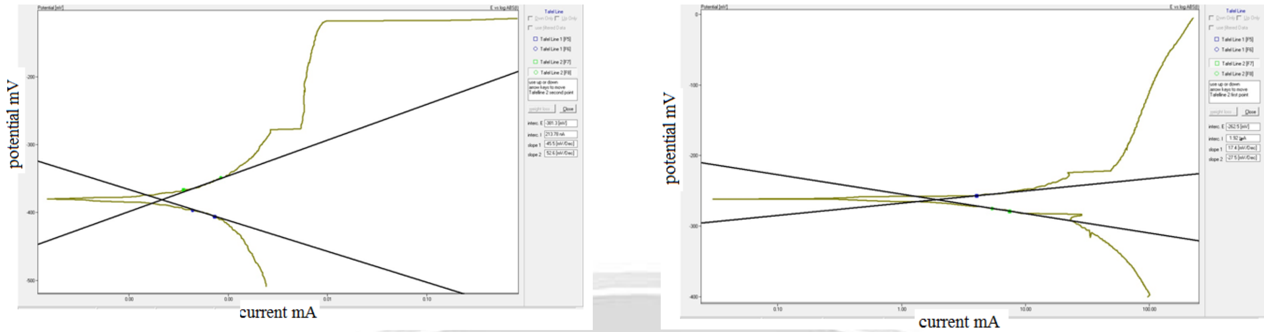

(c)400RF **(d)600RF**

Figure (7): The corrosion test for: (a)bare, (b)200RF, (c)400RF, (d)600RF

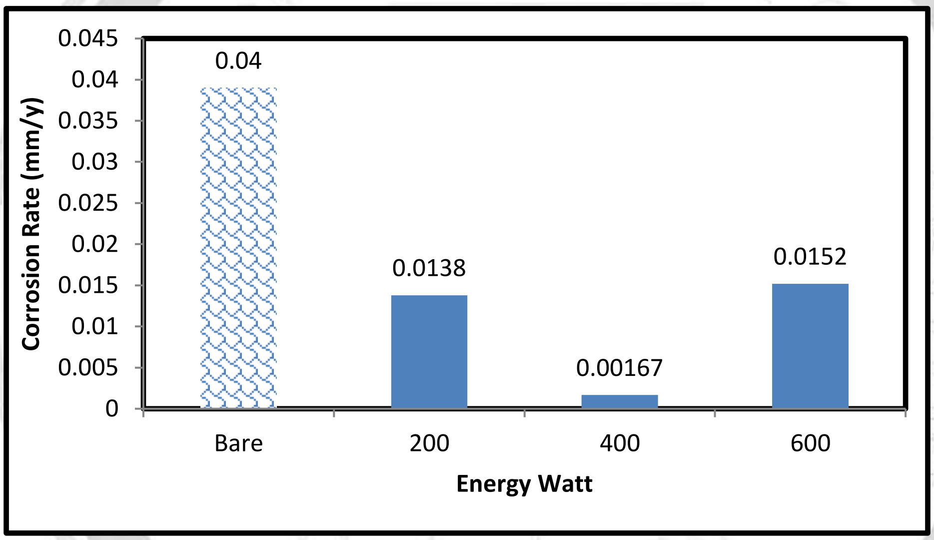

Figure (8): Corrosion rate of deposited film on nitinol after RF sputtering

3.6 MTT(Dimethyl-thiazol-diphenyl-tetrazolium-bromide)Test:

This test to calculate the percentage of cell viability and known the toxicity of the deposited film and the substrate. The bare specimen of nitinol without deposition had the viability percentage of cell as 94.0837% as presented in Figure(9). At low power 200W and high power 600W the percentage of cell viability were 74.70334% and 74.35275% respectively which meant there was percent of toxicity but for 400W the percentage of cell viability was 93.10949% approached the bare specimen. The circumstances of the film deposition at low and high power with different time deposition at the same temperature led to similar toxicity. The plasma formed in RF sputtering effects on nature of film deposition. The appearance of cells after 24 hours as incubation time shown in Figure (10) under microscope.

ISSN: 2616 - 9916 | www.journalofbabylon.com | Journal.eng@uobabylon.edu.iq | info@journalofbabylon.com

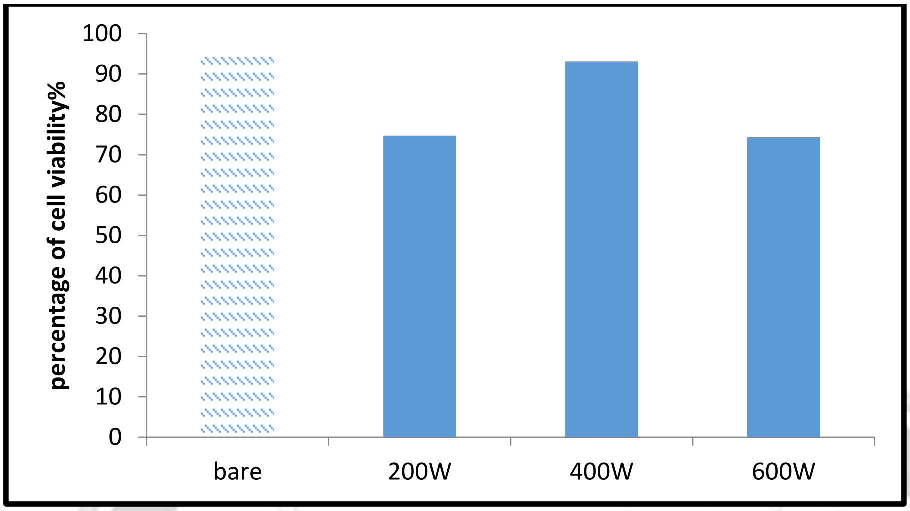

Figure (9): The effect of nitinol after RF sputtering on MDCK cell line (after incubation for 24 hours) versus control group

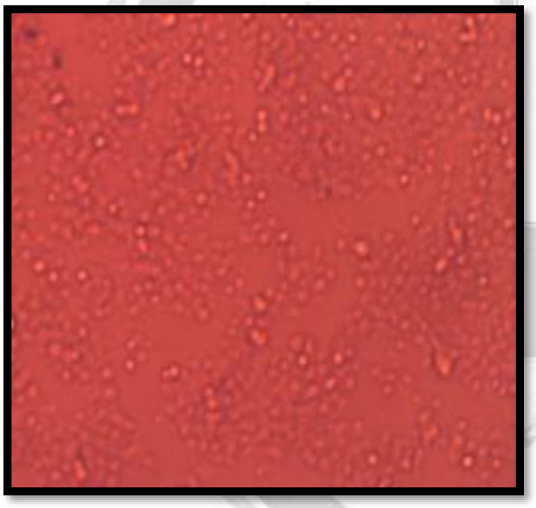

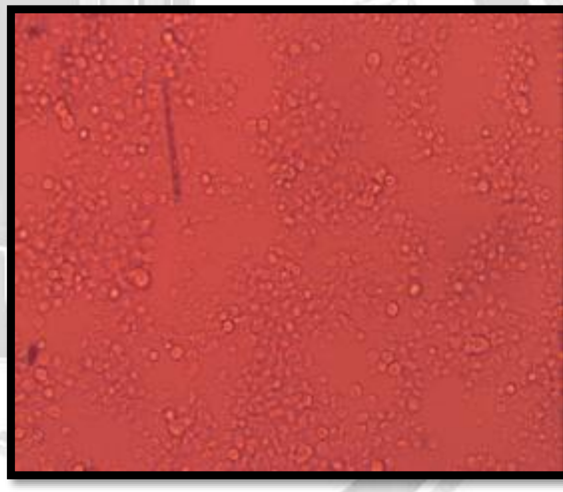

(a) **(b)**

ISSN: 2616 - 9916
www.journalofbabylon.com | Journal.eng@uobabylon.edu.iq | info@journalofbabylon.com

ISSN: 2616 - 9916 | www.journalofbabylon.com | Journal.eng@uobabylon.edu.iq | info@journalofbabylon.com

مجلة جامعة بابل للعلوم الهندسية مجلة جامعة بابل للعلوم الهندسية مجلة جامعة بابل للعلوم الهندسية

(c)

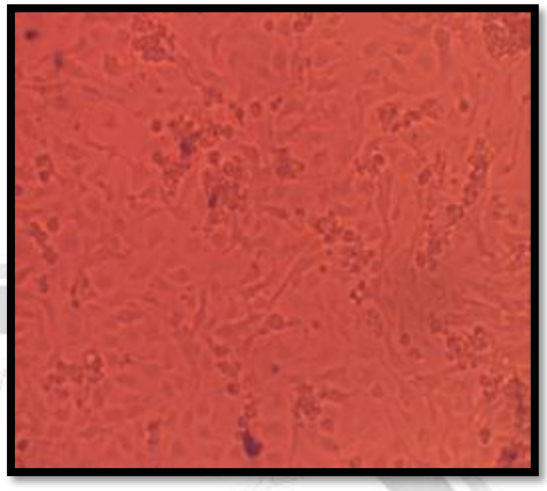

(d)

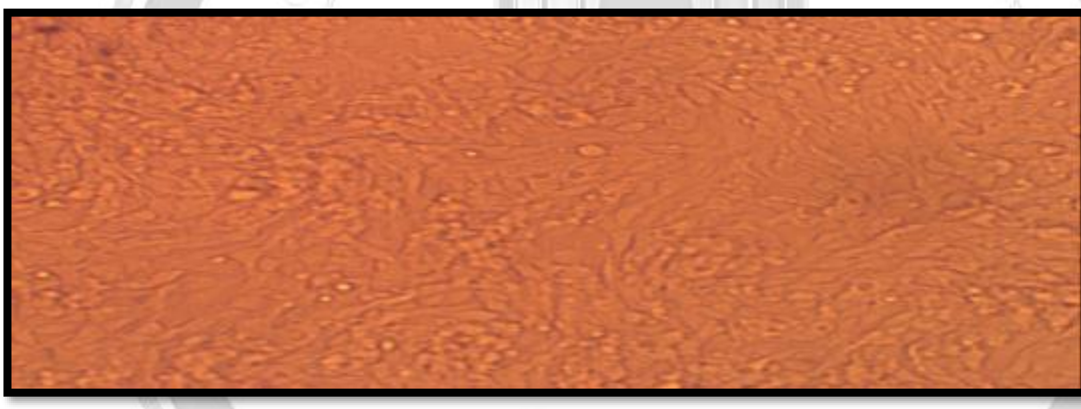

(e)

Figure(10): The appearance of MDCK cells after 24 hours of incubation: (a) 200 RF, (b) 400RF, (c) 600RF, (d) bare, (e) control

4. Genetic Algorithm with Fuzzy Inference System:

To find optimized results for RF sputtering the combination of genetic algorithm and fuzzy inference system as shown in Figure (11).

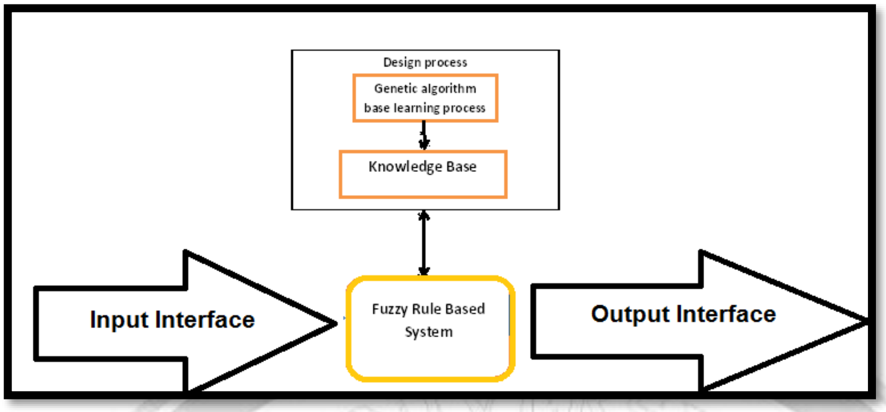

Figure(11): Genetic algorithm with fuzzy inference system[22]

The values of power for RF sputtering were entered as stated and depended on state of machine for sputtering from 200 W to 600W. The calculated values of Vickers hardness entered from the minimum value 362 to maximum value as 660. The friction coefficient limited between 0.3 and 0.47. The corrosion current density changed from 0.12 to 1.076. The cell viability as the other properties changed from 75% to 94%. Figure (12) represents the schematic of input values for properties in the program.

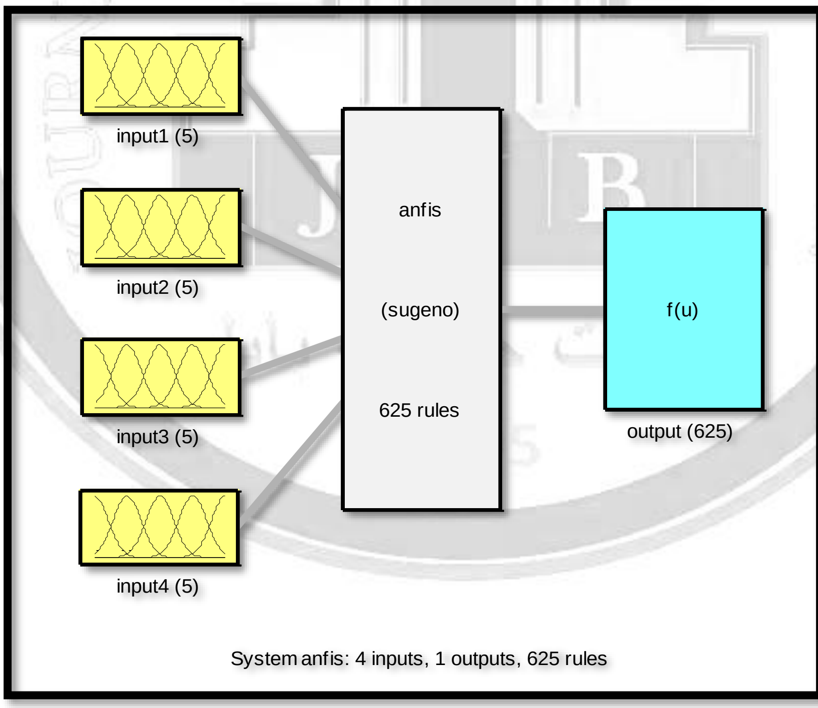

Figure (12) : Schematic of the input function and output

ISSN: 2616 - 9916 | www.journalofbabylon.com | Journal.eng@uobabylon.edu.iq | info@journalofbabylon.com

ARTICLE

JOURNAL OF UNIVERSITY OF BABYLON
For ENGINEERING SCIENCES (JUBES)

Vol.29, No.2.| 2021

After application all steps of genetic algorithm and fuzzy inference system the drawing for degree of membership and each properties were observed in Figures (13).

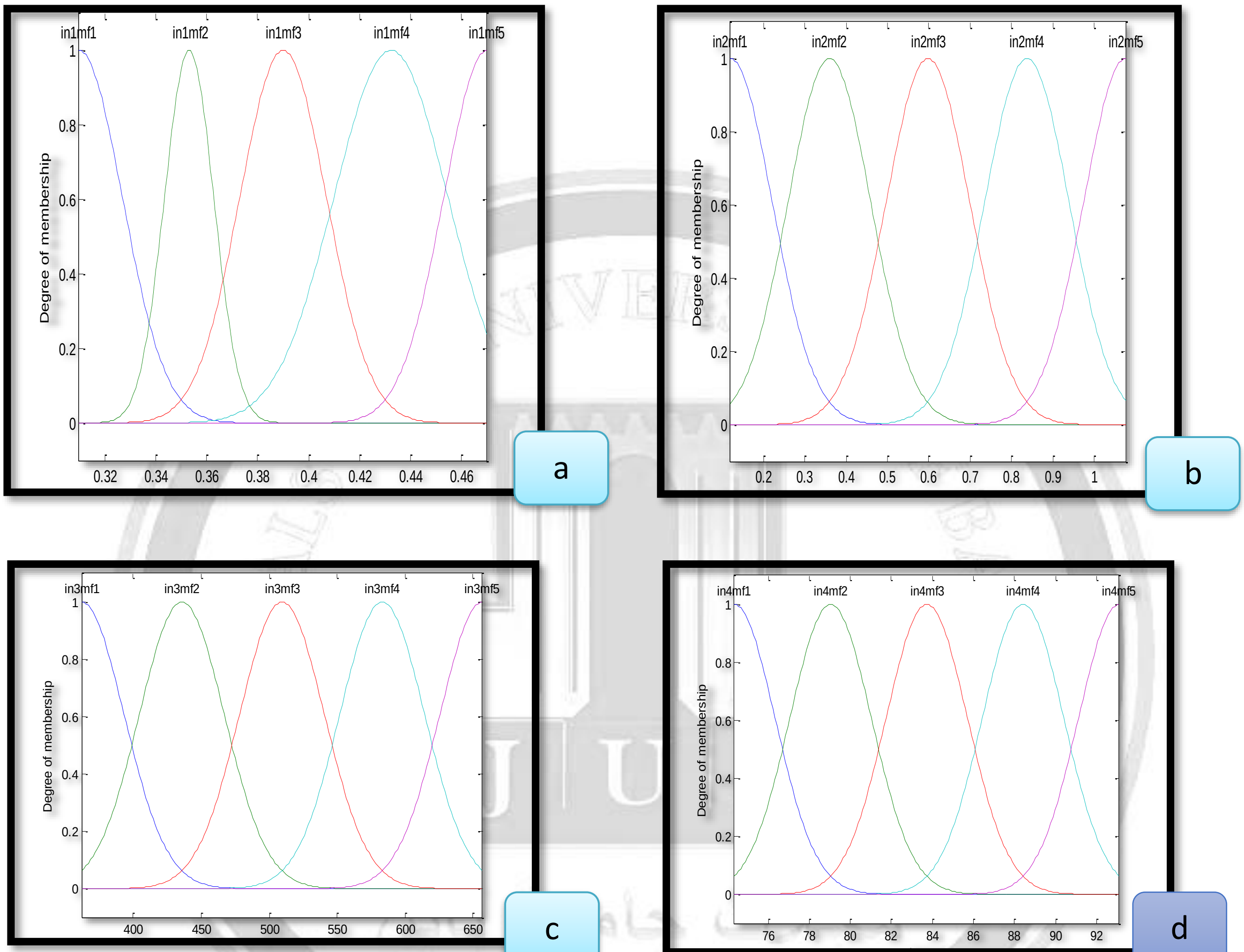

Figure (13): Input values after training: (a)friction coefficient, (b) corrosion current density (c)Vickers hardness, (d) MTT

مجلة جامعة بابل للعلوم الهندسية مجلة جامعة بابل للعلوم الهندسية مجلة جامعة بابل للعلوم الهندسية

info@journalofbabylon.com | Journal.eng@uobabylon.edu.iq | www.journalofbabylon.com | ISSN: 2616 - 9916

Figure (14) represents example of active roles in genetic with fuzzy inference system.

Figure (14): Active rules of FIS(fuzzy inference system)

After application the program , the results as follow in table (2):

Table (2): Results from program of RF sputtering

Number of nodes:	1297
Number of linear parameters	3125
Number of nonlinear parameters	40
Total number of parameters	3165
Number of training data pairs	3
Number of checking data pairs	0
Number of fuzzy rules	625
The optimum value of power	222W
The optimum value of current density of corrosion	0.138µA/cm^2
The optimum value of Friction coefficient	0.2333
The optimum value of MTT	88.8%
The optimum value hardness	666

مجلة جامعة بابل للعلوم الهندسية
ISSN: 2616 - 9916 | www.journalofbabylon.com | Journal.eng@uobabylon.edu.iq | info@journalofbabylon.com

ARTICLE
JOURNAL OF UNIVERSITY OF BABYLON
For ENGINEERING SCIENCES (JUBES)
Vol.29, No.2.| 2021

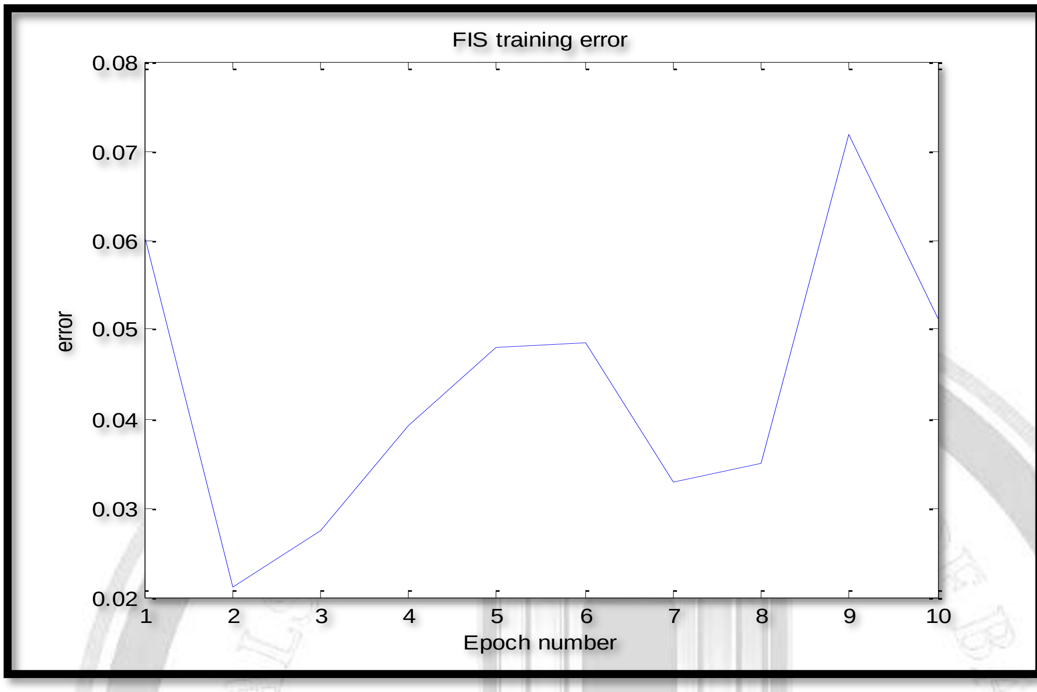

Figure (15) : Fuzzy inference system error of RF sputtering

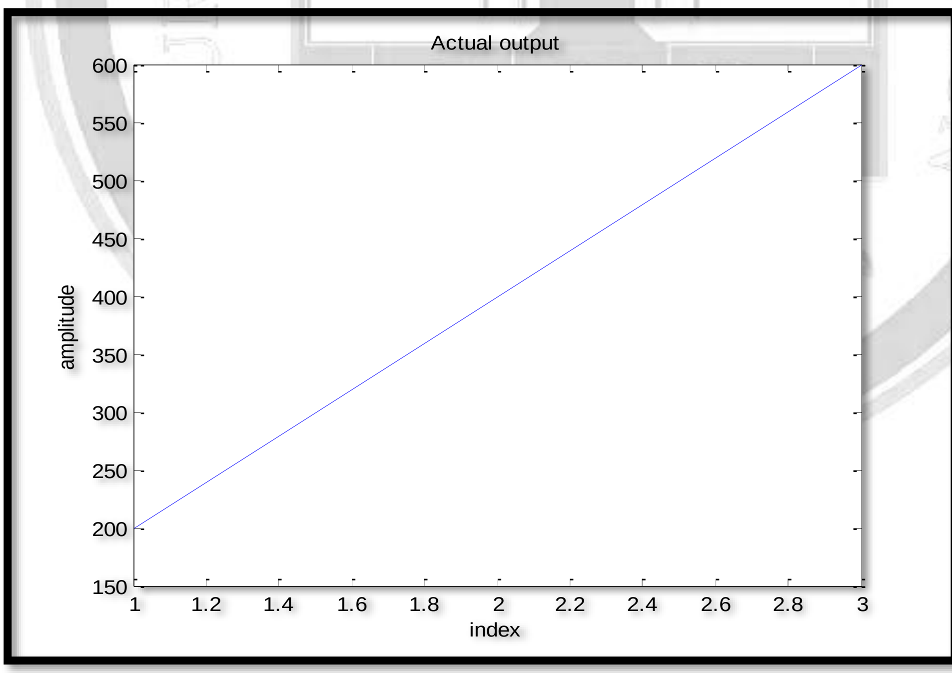

Figure (16): The actual output of RF sputtering

ISSN: 2616 - 9916 www.journalofbabylon.com | Journal.eng@uobabylon.edu.iq | info@journalofbabylon.com

مجلة جامعة بابل للعلوم الهندسية

ISSN: 2616 - 9916 | www.journalofbabylon.com | Journal.eng@uobabylon.edu.iq | info@journalofbabylon.com

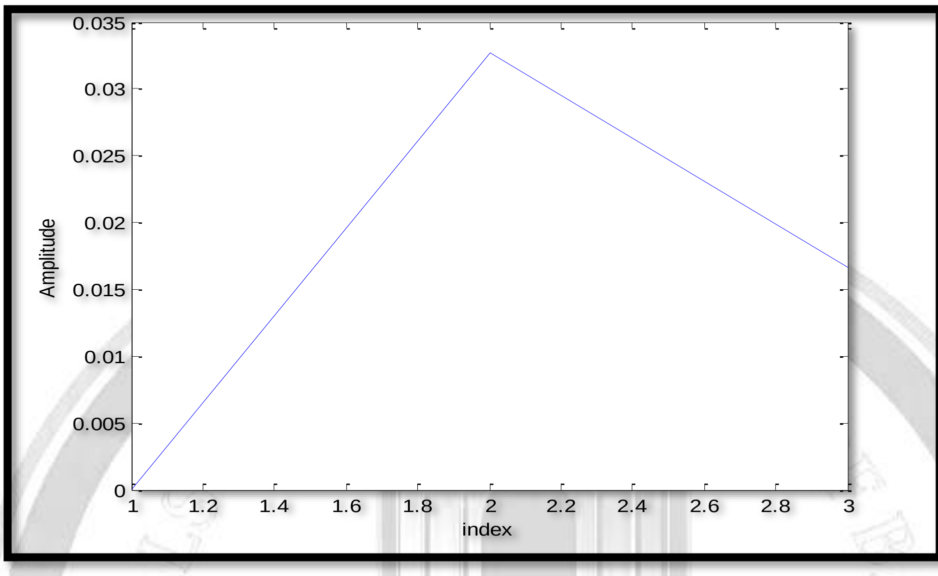

Figure (17): The error between actual and desired output of RF sputtering

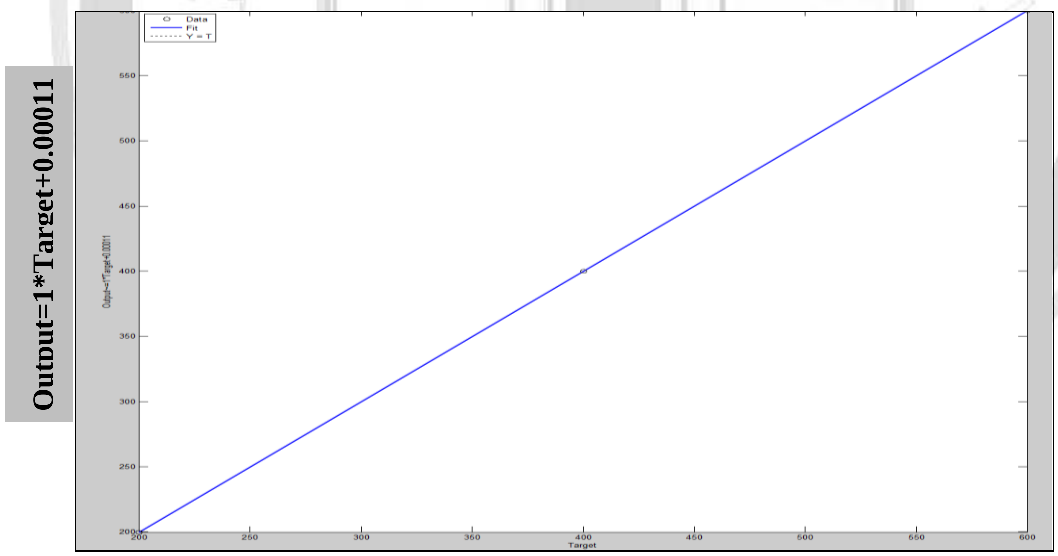

Figure (18): The regression plot of RF sputtering

The comparison the experimental and optimized values listed in table(3). Some of the optimum values corresponding with the specimen after 200W as the corrosion rate with 0.0138mm/y with corrosion density 0.996µm/cm^2 lower than the substrate but higher than the optimized value. The hardness of actual specimen after 200W was 362 lower than the optimized value but higher than the hardness of nitinol alloy. The friction coefficient of this specimen represented as friction coefficient 0.37 higher than the optimized

ISSN: 2616 - 9916 | www.journalofbabylon.com | Journal.eng@uobabylon.edu.iq | info@journalofbabylon.com
مجلة جامعة بابل للعلوم الهندسية

value but the wear rate of it lower than the wear rate of the nitinol alloy alone. From the comparison between actual values and optimized values could be considered the specimen of 200W was the best.

Table (3): The comparison the experimental and optimized values for RF sputtering

Symbol of specimen	Experimental	Optimized
Energy(W)	200	222
hardness	362	666
Current density	0.996	0.138
Cell viability %	74.703	88.8
Friction coefficient	0.37	0.233

5. Conclusions :

1.Deposited films of diamond like carbon DLC after RF sputtering had better properties than the nitinol alloy.

2. Increasing the hardness with increasing the power of RF sputtering.

3.Decreasing the roughness with increasing the power at constant other conditions of process.

4.The values of corrosion rate after deposition decreased to minimum value as 0.001mm/y after 400W.

5.DLC behaved as tribofilm and reduced wear rate to low values after RF sputtering.

6.The maximum value of cell viability raised after 400W with minimum corrosion rate.

7.The optimized value of power with high hardness, low wear rate, high corrosion resistance, low toxicity which means high cell viability was 222W. These results approached to 200W.

6.Refrences:

1. Olayinka, Oluwatosin, Esther Titilayo Akinlabi, Oluseyi Philip Oladijo, et al. "Overview of Thin Film Deposition Techniques", *AIMS Materials Science*, Vol. 6, No. 2, pp. 174–199, 2019.

2. J. Ramsden, D.M. Allen, D. J. Stephenson ,et al. "The Design and Manufacture of Biomedical Surfaces." *Crip Annals-Manufacturing Technology*, Vol.56, No.2, pp.687-711,2007.

3. Andresa,, Baptista , Francisco Silva, Jacobo Porteiro ,et al. " Sputtering Physical Vapour Deposition (PVD) Coatings: A Critical Review on Process Improvement and Market Trend Demands." *Coatings*, Vol.8, No. 402,2018.

4. J. Davis, *Surface Engineering for Corrosion and Wear Resistance*. USA: The Materials Information Society, ASM, Institute of Materials,2001.

5. P. Li., and P.K. Chu. "Thin film Deposition Technologies and Processing of Biomaterials." In *Thin Film Coatings for Biomaterials and Biomedical Applications*. Edited by Hans J Griesser, Elsevier Ltd,2016.

6. L. Freund, and S. Suresh. *Thin Film Materials: Stress ,Defect Formation and Surface Evolution*. Cambridge University Press,1st ed. ,2003.

7.Moriguchi Hideki, Hisanori Ohara, and Masanori Tsujioka. " History and Applications of Diamond-Like Carbon Manufacturing Processes", *SEI Technical Review*,No.82, 2016.

8. R. Parkinson, , Richard J. Balling, John D. Hedengren. *Optimization Methods for Engineering Design Applications and Theory*, Brigham Young University,2nd ed,2018.

9.Ross, J. " *Fuzzy Logic with Engineering Applications*." Wiley,4thed,2017.

10 Praveenkumar Kiranagi, and V. R. Kabadi. "Realistic Approach to Pin –on-Disc Wear Testing Measurement." *International Journal of Advanced Production and Industrial Engineering*,Vol.610,pp.47-53, 2017.

11. A. Ellor , and John Repp. "Electrochemical Test and Tafel Extrapolation Polarization Resistance." In *Corrosion Test and Standards Application and Interpretation*. Edited Robert Baboian , 2nd ed, USA:ASTM Stock number is MNL20,2005.

12. Andrew, Michael,. "Enhancing Corrosion Performance of Laser Modified NiTi Shape Memory Alloy." MSc Diss. *University of Waterloo*, Ontario, Canada,2014.

13. Merlen , Alexandre, Josephus Gerardus Buijnsters and Cedric Pardanaud. "A Guide to and Review of the Use of Multi-wavelength Raman Spectroscopy for Characterizing Defective Aromatic Carbon Solids: from Graphene to Amorphous Carbons." *Coatings*, Vol.7, No.153, 2017.

14. Giulia, Fiaschi, Alberto Rota, Antonio Ballestrazzi , et al. "A Chemical, Mechanical, and Tribological Analysis of DLC Coatings Deposited by Magnetron Sputtering", *Lubricants*, MDPI, Vol. 38, No.7,2019.

15. I. Branzoi, M. Iordoc, F. Branzoi , etal. "Influence of Diamond-Like Carbon Coating on The Corrosion Resistance of The Nitinol Shape Memory Alloy." *Surface and Interface Analysis*, John Wiley & Sons, Vol.42,pp. 502–509,2010.

16. Don, Kaewdook, Akito Takasaki, and Tosihiro Okabe. "Deposition of Amorphous Carbon Thin Films by RF Magnetorn Sputtering using Woodceramics as Target." *Transformation Materials Research* ,Japan,Vol.39, No.1, pp39-42,2014.

17.Huang, Meidong, Xueqian Zhang , Peiling Ke, et al. "Graphite-like Carbon Films by High Power Impulse Magnetron Sputtering." *Applied Surface Science*, Elsevier, Vol.283, pp.321-326,2013.

18. Xi, Yeting, Yanyun Bai, and Kewei Gao. "Residual Stress and Microstructure Effects on Mechanical, Tribological and Electrical Properties of TiN Coating on 304 Stainless Steel." *Ceramic International*, Elsevier, Vol.44,pp.15851-15858, 2018.

19. Teresca, Vieira, Jose Castanho, and Cristina Louro. " Hard Coatings Based on Metal Nitrides, Metal Carbides and Nanocomposite Materials: PVD Process and Properties." In *Materials Surface Processing by Directed Energy Techniques*. Edited by Yves Pauleau, Great Britain: Elsevier Ltd, 2006.

20. Dabing, Luo, "Selection of Coatings for Tribological Applications.", PhD Diss. *Lyon University*, France,2009.

21. Luo., Quanshun. "Tribofilms in Solid Lubricants." *In Encyclopedia of Tribology*. Edited by Wang Q. Jane and Chung Yip-Wah, Sheffield Hallam University Research Archive (SHURA), Springer,2013.. http://shura.shu.ac.uk/information.html.

22. Azar. Zafari, "Developing a Fuzzy Inference System by Using Genetic Algorithms and Expert Knowledge.", MSc Diss. *University of Twente* ,2014.

ISSN: 2616 - 9916 | www.journalofbabylon.com | Journal.eng@uobabylon.edu.iq | info@journalofbabylon.com

ARTICLE
JOURNAL OF UNIVERSITY OF BABYLON
For ENGINEERING SCIENCES (JUBES)
Vol.29, No.2.| 2021

ISSN: 2616 - 9916 | www.journalofbabylon.com | Journal.eng@uobabylon.edu.iq | info@journalofbabylon.com

"الامثلية باستخدام التشتيت بالترددات الراديوية للكرافيت على النتنول"

زينب فاضل كاظم اقبال محمد سعيد حيدر عبد حسن الجبوري

قسم هندسة المعادن، كلية هندسة المواد، جامعة بابل، بابل، العراق

E-mail: mat.zainab.fadhil@uobabylon.edu.iq

الخلاصة:

الاداء العالي الذي تظهره سبيكة النيكل–تيتانيوم لكونها سبيكة ذاكرة للشكل وامتلاكها لخاصية المرونة الفائقة والتوافية الحياتية ادى الى انتشار واسع لهذه السبيكة كمادة هندسية. تم ترسيب طبقة رقيقة على سبيكة نيكل–تيتانيوم باستخدام هدف من الكرافيت وعن طريق استخدام التشتيت بالاشعة الراديوية باعتبارها احدى طرق الترسيب الفيزيائي للبخار. قياس التحسن في الصلادة ومعدل البلى والخشونة ومعدل التاكل ومعدل التواجد الحيوي للخلايا قبل وبعد الترسيب. ثلاث قيم للطاقة تم استخدامها وهي (٢٠٠واط، ٤٠٠واط، ٦٠٠واط). اعتبرت الطبقة المترسبة عبارة عن الماس المشابه للكاربون بالاعتماد على القيم الناتجة من مطياف رامان. يتميز الماس المشابه للكاربون بكونه مضاد للبكتيريا ويمتلك مقاومة عالية للتاكل ومقاومة جيدة للبلى ومعامل احتكاك منخفض وصلادة عالية. اعلى صلادة تم الحصول عليها عند استخدام طاقة الترسيب ٦٠٠واط ومقدارها ٦٥٧ مع معدل بلى منخفض ومقداره ٧،٣٤*١٠$^{-8}$ غم/سم. اعلى مقاومة للتاكل تم الحصول عليها بعد استخدام ٤٠٠واط وكانت ٠،٠٠١ملم/سنة واعلى مقدار من الخلايا الحية وهو ٩٣،١١%. النتائج الامثل من خلال الخوارزمية الجينية مع نظام الاستدلال المضبب ب مقدار٢٢٢واط مع صلادة فيكرز بمقدار ٦٦٦ وكثافة تيار التاكل ٠،١٣٨ ومقدار الخلايا الحية ٨٨،٨.

الكلمات الدالة: سبيكةالنتنول، التشتيت، التردد الراديوي، الترسيب، الهدف، الكرافيت.